Suppressing homoclinic chaos for a weak periodically excited non-smooth oscillator

Shuangbao Li[a,*], Xixi Ma[a], Xiaoli Bian[b], Siu-Kai Lai[c,d], Wei Zhang[e,*]

[a]*College of Science, Civil Aviation University of China, Tianjin 300300, China*

[b]*School of Science, Tianjin University of Technology and Education, Tianjin 300222, China*

[c] *Department of Civil and Environmental Engineering, The Hong Kong Polytechnic University, Kowloon, Hongkong, China*

[d] *The Hong Kong Polytechnic University Shenzhen Research Institute, Shenzhen, China*

[e]*College of Aeronautical Engineering, Civil Aviation University of China, Tianjin, 300300, China*

Abstract

In this work, some new effective methods for suppressing homoclinic chaos in a weak periodically excited non-smooth oscillator are studied, and the main idea is to modify slightly the Melnikov function such that the zeros are eliminated. Firstly, a general form of planar piecewise-smooth oscillators is given to approximatively model many nonlinear restoring force of smooth oscillators subjected to all kinds of damping and periodic excitations. In the absence of controls, the Melnikov method for non-smooth homoclinic trajectories within the framework of a piecewise-smooth oscillator is briefly introduced without detailed derivation. This analytical tool is useful to detect the threshold of parameters for the existence of homoclinic chaos in the non-smooth oscillator. After some methods of state feedback control, self-adaptive control and parametric excitations control are respectively considered, sufficient criteria for suppressing homoclinic chaos are derived by employing the Melnikov function of non-smooth systems. Finally, the effectiveness of strategies for suppressing homoclinic chaos is analytically and numerically demonstrated through a specific example.

Keywords: Melnikov method; non-smooth oscillators; homoclinic chaos; suppressing chaos.

1. Introduction

Stimulated by the development in control theory and mechanical engineering, the study of non-smooth or even discontinuous dynamical systems has recently received extensive attention [1-7]. In actual engineering systems, there are usually a large number of non-smooth factors such as gap [8], impact [9], dry friction [10], variable stiffness [11], switching in control and electronic circuit [12-14] and so on. They are mainly determined by constraints, constitutive relations and control methods. Planar non-smooth periodic perturbation systems are often employed to approximatively model many nonlinear restoring force of smooth oscillators under all kinds of damping effects and periodic excitations, hence, it is an interesting and challenging topic to study the mechanism and control of chaos by geometrical or analytical techniques for this class of systems.

From the view of controlling purpose, chaos control can be divided into chaos suppression and chaos generation, also known as anti-control of chaos. From the control principle, chaos control may be divided into feedback control and non-feedback control [15]. In 1990, Ott, Grebogi and Yorke [16] has put forward a typical feedback control of chaos, also named as OGY method. Many scholars have made many improvements and further generalizations to OGY method [17-20]. Feedback control methods require continuous and accurate monitoring of system variables and

*Corresponding author.
Email address: shuangbaoli@yeah.net (S. B. Li), XixiMa2009Y@163.com (X. X. Ma), bianxiaoli@yeah.net (X. L. Bian), sk.lai@polyu.edu.hk(S. K. Lai), weizha_2001@163.com(W. Zhang).

real-time calculation of perturbation feedback variables, it is often difficult to implement in reality. At the same time, non-feedback control methods can often make up for their shortcomings, such as constant excitation control [21], impulse excitation control [22] and weak harmonic perturbations control with relative phase [23-25]. The research in [26] shows that resonant excitations are effective ways to drive a nonlinear oscillator towards a given target dynamics. Braiman et al. [27] further obtained that an additional periodic external excitation was really an effective way for controlling chaos and provided the numerical evidence for the effectiveness of the control through a periodically driven pendulum.

The Melnikov method is well know as a rare analytical tool for detecting the occurrence and parametric threshold of chaos induced by the existence of transverse homoclinic solutions for time-periodic perturbed systems. In the following we will briefly review the development of the Melnikov method from smooth dynamical systems to discontinuous dynamical systems. In 1963, the classical Melnikov method for planar smooth periodic perturbed systems was first proposed by Melnikov in [28]. The key idea of this method is to study the transverse homoclinic points of the corresponding two-dimensional Poincaré map. Since the Melnikov method was studied and employed to study homoclinic tangencies of the Duffing equation with negative stiffness under the action of weak periodic forcing and weak damping [29], it has been well known as the analytical method for studying homoclinic chaos and global bifurcations. The Melnikov method in the case of high-dimensional nonlinear systems with action-angle variables was also developed by Wiggins, see the monographs [30]. Zhang et al. [31, 32] extended Melnikov method for non-autonomous nonlinear dynamical systems and application to multi-pulse chaotic dynamics. To further investigate the bifurcation characteristics and homoclinic chaos in non-smooth or even discontinuous dynamical systems, many scholars attempted to extend the Melnikov method within an appropriate framework. For the simple case of non-smooth trajectories crossing switching manifolds, Kunze [2] first presented a basic geometrical approach of extending the Melnikov method for a concrete non-smooth dynamical system under time-periodic perturbations, but there is no detailed proof process. Then, Kukucka [33] and Shi et al. [34] further derived the Melnikov functions in detail for planar discontinuous systems with only one switching manifold. However, the derived Melnikov function contains difference items which are induced by the discontinuous features of vectors on the switching line, its application in engineering is limited because of the difficulty of calculation. The Melnikov method for a kind of impact oscillators was also studied by Du and Zhang [35] and Xu et al. [36] by choosing different normal line on the Poincaré section, respectively. Granados et al. [37] has employed a reset map to describe the orbital collision with switching manifolds and proposed the Melnikov theory for analyzing subharmonic and heteroclinic trajectories in a planar non-smooth systems under weak time-periodic perturbations. Battelli and Fečkan. [38-40] used alternative techniques to obtain Melnikov functions for high-dimensional discontinuous systems with one switching manifold, but the intuition of geometry is not obvious. Tian et al. [41] also derived the Melnikov function and studied the chaotic threshold for a non-smooth pendulum with different impulsive excitations realized by collision with a rigid wall. In order to study the global dynamics of discontinuous systems with geometric visualization and overcome the difficulties in calculation and applications, more recently Li et al. [42-47] employed a geometrical approach and different proof to systematically derive the Melnikov function in a simple form for trajectories transversally crossing or instantaneously jumping on switching manifolds.

Many scholars have made great efforts in the field of the controlling of homoclinic chaos and achieved some results based on the classical Melnikov method presented in [28-30]. Chaos control by means of the Melnikov method began in about 1990. Indeed, Lima et al. [48] employed the Melnikov method to demonstrate that resonant parametric perturbations in the Duffing-Holmes equation was effective to suppress chaos. Rajasekar [49] considered a Duffing-van der-Pol oscillator subjected to weak periodic perturbations and studied the parametric regimes for controlling of chaos by the classical Melnikov method. Lenci et al. [50] employed the Melnikov method and studied the optimal forcing in the Duffing oscillator to avoid homoclinic tangencies so that chaotic dynamics was suppressed. Leung and Liu [51, 52] proposed several methods and criteria of controlling chaos through adding controls such that the new Melnikov function no longer has zeros. Chacón has systematically summarized the Melnikov method and control mechanism of weak periodic excitations for suppressing homoclinic/heteroclinic chaos in their monographs [53]. Yang et al. [54] considered a parametrically and externally excited pendulum and investigated the analytical and numerical evidences of chaos control by using the Melnikov method. Jimenez et al. [55] further investigated homoclinic chaos and suppression in the Duffing system by applying a class of discontinuous periodic parametric perturbations based on the Melnikov method. Li et al. [56] studied chaos control of a piecewise smooth oscillator under small parametrical perturbations. In 2018, Du et al. [57] considered a fractional-order deflection Duffing oscil-

lator and studied the strategies of adding excitations by the classical Melnikov method for suppressing chaos. More recently, the key issue of relative phase has been explored both experimentally and theoretically through the Melnikov analysis in the duffing oscillator by Martínez and Chacón et al. [58, 59].

How to study the mechanism and control of chaos for non-smooth systems by geometrical or analytical techniques is an interesting and challenging topic. In this work, we employ the developed Melnikov function for time-periodic perturbed planar non-smooth or even discontinuous systems to study some simple and easy to implement control methods of homoclinic chaos. We give a general form of planar piecewise smooth systems to approximatively model many nonlinear restoring force of smooth oscillators under weak damping and periodic excitations. We first assume that there exist homoclinic solutions which are piecewise defined and transversally cross two switching manifolds in the unperturbed system, that is, there are no action of damping and excitations. Then, the Melnikov method of planar non-smooth systems is employed to detect the parametric threshold for homoclinic chaos for the time-periodic perturbed system. When some methods of state feedback control, self-adaptive control and parametric excitations control [51, 52] are respectively considered, sufficient criteria for suppressing homoclinic chaos are derived. The basic mechanism is to detect the threshold of parameters such that the modified Melnikov function's zeros are eliminated.

The structure of this paper is as below. In Sect. 2, a brief introduction to the Melnikov method is provided for a non-smooth oscillator under weak time-periodic perturbation. In Sect. 3, some control methods of state feedback control, self-adaptive control and parametric excitations control are respectively considered and sufficient criteria for suppressing homoclinic chaos are derived. In Sect. 4, global bifurcations, homoclinic chaos and the strategies for suppressing chaos are analyzed in detail for a concrete oscillator under external excitation by using the Melnikov method. Numerical results for a specific oscillator by adjusting control parameters are also shown to verify the feasibility of the presented chaos control method. Finally, the conclusions are given.

2. A brief introduction of Melnikov method for non-smooth oscillators

2.1. Non-smooth oscillators

In this section, we will briefly introduce the derivation of the Melnikov method within the framework of a piecewise described non-smooth oscillator. The dynamical equation with a dimensionless general form is shown as follows:

$$\ddot{x} + f(x) + \epsilon\delta g(x, \dot{x}) = \epsilon f \cos \Omega t, \tag{1}$$

where $0 < \epsilon \ll 1$ is a small perturbation parameter of this systems, $\epsilon\delta g(x, \dot{x})$ and $\epsilon f \cos \Omega t$ respectively denote weak dampings and weak external periodic excitations, $f(x)$ is a piecewise defined restoring force of the form

$$f(x) = \begin{cases} f_+(x), & |x| > a, \\ f_-(x), & |x| < a, \end{cases} \tag{2}$$

where $a > 0$ is a constant used to define the switching manifolds $\Sigma_\pm = \{(\pm a, y) | y \in \mathbb{R}\}$.

As we all know that $f(x)$ can be used to express restoring forces in actual mechanical models. There are two reasons to study the aforementioned piecewise smooth systems. One reason is that elastic restoring forces in many mechanical elastic impact systems are often described by piecewise-defined functions. For instance, the restoring force is piecewise linear for an unilateral elastic impact model studied in [60]. A bilateral elastic impact model shown in Fig.1 consists of a slender block with mass M, attached to two linear springs with stiffness K_1 and two linear dashpots of damping factor C. When the system is subjected to a periodic external excitation $F \cos \omega t$, this block M moves to the left or right. When the motion distance exceeds a certain value X_0, the second spring of stiffness K_2 will contact the block M. Without loss of general assumption that $X_0 > 0$, all springs produce an overall restoring force which is defined by a piecewise linear function of the form

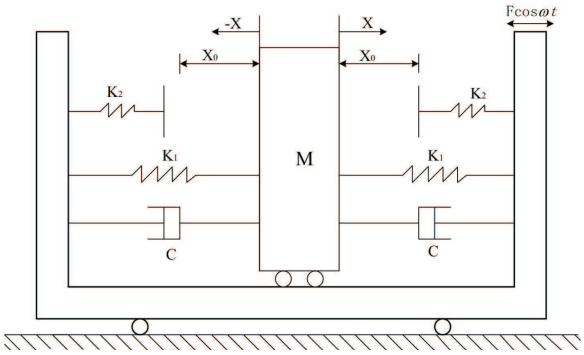

Figure 1: An elastic impact oscillator.

$$f(x) = \begin{cases} 2K_1X, & |X| < X_0, \\ 2K_1X + K_2(X - sign(X)X_0), & |X| \geq X_0. \end{cases} \tag{3}$$

such that the equation of motion for the block can be written as

$$M\ddot{X} + f(X) + 2\epsilon C\dot{X} = \epsilon F \cos \Omega t. \tag{4}$$

The other reason for considering the general system (1)-(2) is that the restoring force is described by smooth irrational [61, 62] or more complex functions in many nonlinear mechanical models. In most cases, it is difficult to analyze the dynamic behavior through analytical methods. Therefore, piecewise linear approximation is often an effective way to solve such problems. For example, a smooth irrational function is employed to describe the restoring force in a simple mechanical model with geometrical nonlinearity presented in [61] as shown in Fig.2, the dimensionless equation of motion may be written as follows:

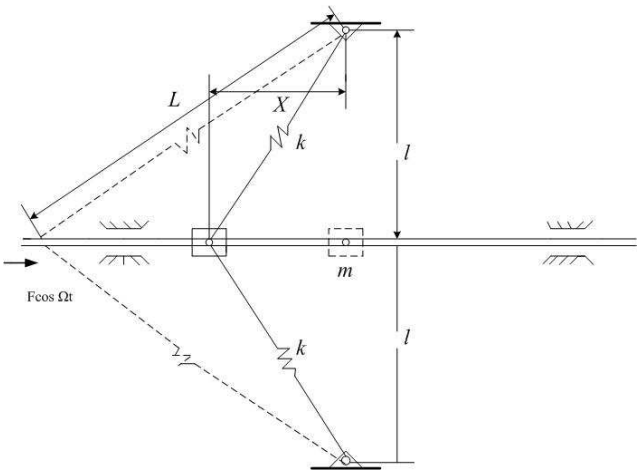

Figure 2: A simple oscillator with irrational restoring forces.

$$\ddot{x} + \omega^2 x(1 - \frac{1}{\sqrt{x^2 + \alpha^2}}) + \epsilon\delta\dot{x} = \varepsilon f \cos \Omega t, \tag{5}$$

where $\alpha = \frac{l}{L}$, when $\varepsilon = 0$, the irrational restoring force can be written as:

$$f(x) = -\omega^2 x(1 - \frac{1}{\sqrt{x^2 + \alpha^2}}). \tag{6}$$

Direct analysis of dynamics for the aforementioned systems by analytical methods is very difficult because of the limitation of elementary functions. The authors in [61] presented an idealized linear approximation for the restoring forces $f(x)$ in the case of $\alpha \in (0, 1)$ written of the form

$$f(x) = \begin{cases} \omega_1^2 x, & |x| \le x_0, \\ -\omega_2^2(x - sign(x)\omega_2), & |x| > x_0, \end{cases} \tag{7}$$

where $\omega_1^2 = (1-\alpha)/\alpha, \omega_2^2 = (1-\alpha^2)$ and $x = x_0$ is the switching line for the ideal piecewise linear restoring forces obtained by

$$x_0 = \frac{\alpha(1+\alpha)\sqrt{1-\alpha^2}}{1+\alpha+\alpha^2}.$$

A idealized piecewise linear approximation to the theoretical restoring force is shown in the following Figure 3 when the parameter α is chosen as $\alpha = 0.5$.

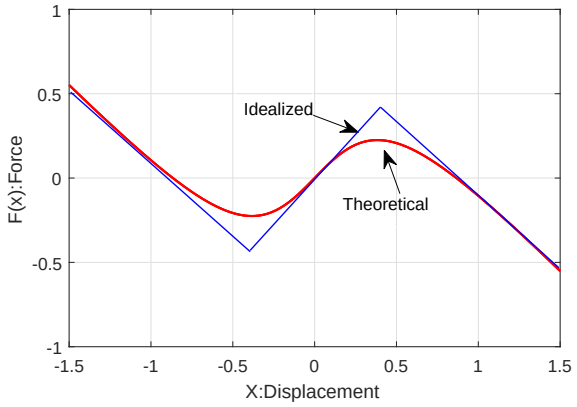

Figure 3: An idealized piecewise linear approximation to the theoretical restoring force

2.2. Melnikov function for piecewise smooth homoclinic orbits

In this paper, we briefly introduce the Melnikov method for non-smooth oscillators. Firstly, we define the switching manifolds $\Sigma_\pm$ which divide the state-space $\mathbb{R}^2$ into S_- and S_+ such that $\mathbb{R}^2 = S_- \cup S_+ \cup \Sigma_\pm$. The subsets S_- , S_+ and the switching manifolds $\Sigma_\pm$ can be written as:

$$\begin{aligned} S_+ &= \{(x, y) \in \mathbb{R}^2 \mid |x| > a\}, \\ S_- &= \{(x, y) \in \mathbb{R}^2 \mid |x| < a\}, \\ \Sigma_\pm &= \{(x, y) \in \mathbb{R}^2 \mid x = \pm a\}. \end{aligned} \tag{8}$$

It is necessary to note that the normal of the switching manifolds $\Sigma_\pm$ is expressed of the form

$$\mathbf{n} = \mathbf{n}(x, y) = (1, 0), \ (x, y) \in \Sigma_\pm.$$

The dynamical equation of the piecewise smooth oscillator described by Eq. (1) can be rewritten as an equivalent systems of the form

$$\begin{cases} \dot{x} = y, \\ \dot{y} = -f_+(x) - \epsilon\delta g(x, y) + \epsilon f \cos \Omega t, & |x| > a, \\ \dot{x} = y, \\ \dot{y} = -f_-(x) - \epsilon\delta g(x, y) + \epsilon f \cos \Omega t, & |x| < a. \end{cases} \tag{9}$$

By setting $\epsilon = 0$, we obtain a unperturbed Hamiltonian system of the form

$$\begin{cases} \dot{x} = y = \partial H_+(x,y)/\partial y, \\ \dot{y} = -f_+(x) = -\partial H_+(x,y)/\partial x, & |x| > a, \\ \dot{x} = y = \partial H_-(x,y)/\partial y, \\ \dot{y} = -f_-(x) = -\partial H_-(x,y)/\partial x, & |x| < a. \end{cases} \tag{10}$$

where the Hamiltonian functions $H_\pm(x,y)$ are expressed of the form

$$\begin{cases} H_+(x,y) = \frac{1}{2}y^2 + \int_0^x f_+(s)ds, & (x,y) \in S_+, \\ H_-(x,y) = \frac{1}{2}y^2 + \int_0^x f_-(s)ds, & (x,y) \in S_-. \end{cases} \tag{11}$$

We first assume that the Hamiltonian functions $H_\pm \in C^r(\mathbb{R}^2, \mathbb{R})$, with $r \geq 1$,and the weak damping $\epsilon\delta g(x,\dot{x})$ is also assumed to be enough smooth in the disjoint zone S_+ and S_-. Without loss of generality, we may assume that the geometrical structure of the system (10) is topologically equivalent to Figure 4. In order to further describe the Melnikov method, the following geometrical assumption of homoclinic structure is necessary and given as follows:

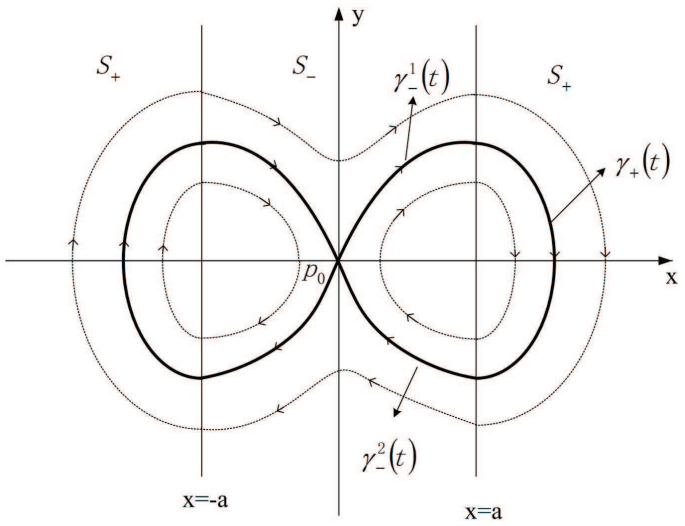

Figure 4: phase portrait of unperturbed system.

Assumption 1. *The unperturbed system (10) has a hyperbolic saddle point $p_0 \in S_-$ and a pair of solutions homoclinic to p_0. The right homoclinic trajectory $\gamma(t)$ transversally crosses the switching manifolds $\Sigma_\pm$ twice such that the three branches can be piecewise expressed of the form*

$$\gamma(t) = \begin{cases} \gamma_-^1(t) = (x_-^1(t), y_-^1(t)) \in S_-, & for\, t < -T, \\ \gamma_+(t) = (x_+(t), y_+(t)) \in S_+, & for\ -T < t < T, \\ \gamma_-^2(t) = (x_-^2(t), y_-^2(t)) \in S_-, & for\, t > T \end{cases} \tag{12}$$

satisfying $\gamma_-^1(-T) = \gamma_+(-T) = (a, y_0) \in \Sigma_+$ and $\gamma_-^2(T) = \gamma_+(T) = (a, -y_0) \in \Sigma_+$, where y_0 is the ordinate of the intersection of the switching manifolds and the homoclinic orbit.

When the weak damping $\epsilon\delta g(x,\dot{x})$ and the weak forcing$\epsilon f \cos\Omega t$ come into play in the unperturbed system, the homoclinic orbits may be broken and homoclinic chaos will occur when the stable and unstable manifolds of the perturbed systems intersect transversally. Therefore, we will discuss the thresholds of parameters for homoclinic

chaos by applying the Melnikov method presented in [42]. We can use the Hamiltonian function $H_+(x, y)$ to measure the distance between stable manifolds and unstable manifolds for system (9) as we did in [42, 45, 46] for discontinuous systems. The basic idea is to extend the vector fields and find the relationship of the perturbed solutions on both sides of the switched manifold by introducing a transfer matrix. Here, we omit the details of the derivation and give the corresponding non-smooth Melnikov functions as follows:

$$\begin{aligned} M_1(\theta_0) =& \frac{n(\gamma(-T)) \cdot \dot{\gamma}_+(-T)}{n(\gamma(-T)) \cdot \dot{\gamma}_-^1(-T)} \int_{-\infty}^{-T} y_-^1(t) \cdot (-\delta g(\gamma_-^1(t)) + f \cos \Omega(t + \theta_0))dt \\ &+ \int_{-T}^{T} y_+(t) \cdot (-\delta g(\gamma_+(t)) + f \cos \Omega(t + \theta_0))dt \\ &+ \frac{n(\gamma(T)) \cdot \dot{\gamma}_+(T)}{n(\gamma(T)) \cdot \dot{\gamma}_-^2(T)} \int_{T}^{+\infty} y_-^2(t) \cdot (-\delta g(\gamma_-^2(t)) + f \cos \Omega(t + \theta_0))dt. \end{aligned} \tag{13}$$

Notice that $\mathbf{n}(\mathbf{x}, \mathbf{y}) = (1, 0)$ as the normal of the switching manifold Σ_+ makes

$$\begin{aligned} \frac{n(\gamma(-T)) \cdot \dot{\gamma}_+(-T)}{n(\gamma(-T)) \cdot \dot{\gamma}_-^1(-T)} &= \frac{(1, 0) \cdot (y_0, -f_+(a))}{(1, 0) \cdot (y_0, -f_-(a))} = \frac{y_0}{y_0} = 1, \\ \frac{n(\gamma(T)) \cdot \dot{\gamma}_+(T)}{n(\gamma(T)) \cdot \dot{\gamma}_-^2(T)} &= \frac{(1, 0) \cdot (-y_0, -f_+(a))}{(1, 0) \cdot (-y_0, -f_-(a))} = \frac{-y_0}{-y_0} = 1. \end{aligned}$$

So the corresponding Melnikov function can be simplified of the form

$$\begin{aligned} M_1(\theta_0) =& \int_{-\infty}^{-T} y_-^1(t) \cdot (-\delta g(\gamma_-^1(t)) + f \cos \Omega(t + \theta_0))dt \\ &+ \int_{-T}^{T} y_+(t)(-\delta g(\gamma_+(t)) + f \cos \Omega(t + \theta_0))dt \\ &+ \int_{T}^{+\infty} y_-^2(t)(-\delta g(\gamma_-^2(t)) + f \cos \Omega(t + \theta_0))dt \\ =& -\delta I_1 - f I_2(\Omega) \sin \Omega\, \theta_0, \end{aligned} \tag{14}$$

where

$$\begin{aligned} I_1 &= \int_{-\infty}^{-T} y_-^1(t) \cdot g(x_-^1(t), y_-^1(t))dt + \int_{-T}^{T} y_+(t) \cdot g(x_+(t), y_+(t))dt + \int_{T}^{+\infty} y_-^2(t) \cdot g(x_-^1(t), y_-^1(t))dt \\ I_2(\Omega) &= \int_{-\infty}^{-T} y_-^1(t) \cdot \sin \Omega t dt + \int_{-T}^{T} y_+(t) \cdot \sin \Omega t dt + \int_{T}^{+\infty} y_-^2(t) \cdot \sin \Omega t dt. \end{aligned} \tag{15}$$

Theorem 1. *Under all the assumptions aforementioned, if the parameters f, δ, Ω satisfy the following condition:*

$$\left| \frac{I_1}{I_2(\Omega)} \right| < \frac{f}{\delta}, \tag{16}$$

then there exists $\theta_0 \in \mathbb{R}$ such that

$$M_1(\theta_0) = 0, \ M_1'(\theta_0) \neq 0,$$

that is, stable manifolds and unstable manifolds intersect transversely near θ_0.

For a rigorous proof of this theorem, readers are referred to [42].

3. Methods of suppressing chaos

In this section, we will consider some criteria and method for suppressing homoclinic chaos through the Melnikov function for systems with non-smooth homoclinic structures. The main idea of the Melnikov method is to study

the existence of transverse homoclinic points of the corresponding two-dimensional Poincar map. Next we consider three-types control methods to modify slightly the non-smooth Melnikov function such that the zeros are eliminated. Eq. (9) with control items is rewritten of the form

$$\begin{cases} \dot{x} = y, \\ \dot{y} = -f_+(x) - \epsilon\delta g(x,y) + \epsilon f_c \cos\Omega t + \epsilon C(x,y,t), & |x| > a, \end{cases}$$
$$\begin{cases} \dot{x} = y, \\ \dot{y} = -f_-(x) - \epsilon\delta g(x,y) + \epsilon f_c \cos\Omega t + \epsilon C(x,y,t), & |x| < a. \end{cases} \tag{17}$$

In this system, $C(x, y, t)$ is the control item divided into three types:

1. $C(x, y, t) = -Ey$, namely, state feedback control;
2. $C(x, y, t) = -Px^2(t)g(x, y)$, namely, self adaptive control;
3. $C(x, y, t) = xf_p \cos(\omega t + \varphi)$, namely, parametric excitations control;

where E, P, f_p are control coefficients. Next we will employ the Melnikov method to describe the conditions of chaos control.

3.1. Control of chaos with state feedback method

Firstly, we consider the state feedback control by adding weak velocity signal $y(t)$ to the system, then the system with state feedback variable becomes

$$\begin{cases} \dot{x} = y, \\ \dot{y} = -f_+(x) - \epsilon\delta g(x,y) + \epsilon f_c \cos\Omega t - \varepsilon E y, & |x| > a, \end{cases}$$
$$\begin{cases} \dot{x} = y, \\ \dot{y} = -f_-(x) - \epsilon\delta g(x,y) + \epsilon f_c \cos\Omega t - \varepsilon E y, & |x| < a. \end{cases} \tag{18}$$

The state feedback control strategy for this perturbed system Eq. (18) will be designed to change chaotic motions into regular periodic motions. By substituting Eq.(18) into Melnikov analysis, we can obtain the Melnikov function including control items of the form

$$\begin{aligned} M(\theta_0) =& M_1(\theta_0) + \int_{-\infty}^{-T} y_-^1(t) \cdot (-Ey_-^1(t))dt \\ &+ \int_{-T}^{T} y_+(t) \cdot (-Ey_+(t))dt \\ &+ \int_{T}^{+\infty} y_-^2(t) \cdot (-Ey_-^2(t))dt \\ =& M_1(\theta_0) - EI_3 \\ =& -\delta I_1 - f_c I_2(\Omega)\sin\Omega\,\theta_0 - EI_3, \end{aligned} \tag{19}$$

where $M_1(\theta_0)$ is shown in Eq. (14) and I_3 is given by

$$I_3 = \int_{-\infty}^{-T} (y_-^1(t))^2 dt + \int_{-T}^{T} (y_+(t))^2 dt + \int_{T}^{+\infty} (y_-^2(t))^2 dt > 0. \tag{20}$$

Theorem 2. *Assume system (9) be chaotic motion under a given initial condition and a set of parameters of systems, if the following parametric inequality holds*

$$|\delta I_1 + EI_3| > f_c |I_2(\Omega)|, \tag{21}$$

then the corresponding Melnikov function $M(\theta_0)$ has no zeros, which implies that the homoclinic chaos appearing in system (9) is suppressed by the state feedback method.

3.2. Control of chaos with self-adaptive method

Now, we let the parameter δ in Eq.(9) be designed to satisfy the self-adaptive control

$$\dot{\delta} = -2Px(t)\dot{x}(t), \tag{22}$$

that is

$$\delta = \delta_0 - Px^2(t), \tag{23}$$

where δ_0 is the value δ in system (9) such that chaotic motions occur. Therefore, the system (9) becomes

$$\begin{cases} \dot{x} = y, \\ \dot{y} = -f_+(x) - \epsilon(\delta_0 + Px^2(t))g(x,y) + \epsilon f_c \cos\Omega t, & |x| > a, \\ \dot{x} = y, \\ \dot{y} = -f_-(x) - \epsilon(\delta_0 + Px^2(t))g(x,y) + \epsilon f_c \cos\Omega t, & |x| < a, \end{cases} \tag{24}$$

After a series of mathematical deductions, we can obtain the Melnikov function $M(\theta_0)$ including control items given by

$$\begin{aligned} M(\theta_0) =& M_1(\theta_0) + \int_{-\infty}^{-T} y_-^1(t) \cdot ((-P(x_-^1(t))^2)g(x_-^1(t), y_-^1(t)))dt \\ &+ \int_{-T}^{T} y_+(t) \cdot ((-P(x_+(t))^2)g(x_+(t), y_+(t)))dt \\ &+ \int_{T}^{+\infty} y_-^2(t) \cdot ((-P(x_-^2(t))^2)g(x_-^2(t), y_-^2(t)))dt \\ =& M_1(\theta_0) - PI_4 \\ =& -\delta_0 I_1 - f_c I_2(\Omega)\sin\Omega\,\theta_0 - PI_4, \end{aligned} \tag{25}$$

where

$$\begin{aligned} I_4 =& \int_{-\infty}^{-T} (x_-^1(t))^2 g(x_-^1(t), y_-^1(t))(y_-^1(t))dt + \int_{-T}^{T} (x_+(t))^2 g(x_+(t), y_+(t))(y_+(t))dt \\ &+ \int_{T}^{+\infty} (x_-^2(t))^2 g(x_-^2(t), y_-^2(t))y_-^2(t)dt. \end{aligned} \tag{26}$$

Theorem 3. *Assume system (9) be chaotic motions under a given initial condition and a set of parameters of systems, if the following parametric inequality holds,*

$$|\delta_0 I_1 + PI_4| > f_c|I_2(\Omega)|, \tag{27}$$

then the corresponding Melnikov function $M(\theta_0)$ has no zeros, which implies that the homoclinic chaos appearing in system (9) is suppressed by the self-adaptive method.

3.3. Control of chaos with adding parametric excitations

We impose the parametric excitations $xf_p\cos(\omega t + \varphi)$ on system (9). Then, the controlled system is rewritten as:

$$\begin{cases} \dot{x} = y, \\ \dot{y} = -f_+(x) - \epsilon\delta g(x)y + \epsilon f_c \cos\Omega t + \epsilon x f_p \cos(\omega t + \varphi), & |x| > a, \\ \dot{x} = y, \\ \dot{y} = -f_-(x) - \epsilon\delta g(x)y + \epsilon f_c \cos\Omega t + \epsilon x f_p \cos(\omega t + \varphi), & |x| < a, \end{cases} \tag{28}$$

where f_c, ω and φ respectively represent the amplitude, the frequency, and the initial phase of the parametric excitations. The Melnikov function $M(\theta_0)$ of system (28) is obtained of the form

$$\begin{aligned} M(\theta_0) =& M_1(\theta_0) + f_p \int_{-\infty}^{-T} x_-^1(t) y_-^1(t) \cos[\omega(t+\theta_0)+\varphi] dt \\ &+ f_p \int_{-T}^{T} x_+(t) y_+(t) \cos[\omega(t+\theta_0)+\varphi] dt \\ &+ f_p \int_{T}^{+\infty} x_-^2(t) y_-^2(t) \cos[\omega(t+\theta_0)+\varphi] dt \\ =& M_1(\theta_0) - f_p \sin(\omega\theta_0+\varphi)[\int_{-\infty}^{-T} x_-^1(t) y_-^1(t) \sin\omega t dt \\ &+ \int_{-T}^{T} x_+(t) y_+(t) \sin\omega t dt + \int_{T}^{+\infty} x_-^2(t) y_-^2(t) \sin\omega t dt] \\ =& -\delta I_1 - f_c I_2(\Omega) \sin\Omega\theta_0 - f_p \sin(\omega\theta_0+\varphi) I_5(\omega), \end{aligned} \tag{29}$$

where

$$I_5(\omega) = \int_{-\infty}^{-T} x_-^1(t) y_-^1(t) \sin\omega t dt + \int_{-T}^{T} x_+(t) y_+(t) \sin\omega t dt + \int_{T}^{+\infty} x_-^2(t) y_-^2(t) \sin\omega t dt. \tag{30}$$

Theorem 4. *If $I_1 > 0$, $I_2(\Omega) > 0$, $I_5(\omega) > 0$, , and f_p satisfies*

$$0 < f_p < \frac{\delta I_1 - f_c I_2(\Omega)}{I_5(\omega)}, \tag{31}$$

then the Melnikov function $M(\theta_0) < 0$ and the homoclinic chaos in system (9) can be suppressed for any phase φ.

Proof: From (29) we can obtain

$$\begin{aligned} M(\theta_0) =& -\delta I_1 - f_c I_2(\Omega) \sin\Omega\theta_0 - f_p \sin(\omega\theta_0+\varphi) I_5(\omega) \\ \le& -\delta I_1 + f_c I_2(\Omega) + f_p I_5(\omega), \end{aligned}$$

when

$$-\delta I_1 + f_c I_2(\Omega) + f_p I_5(\omega) < 0,$$

that is

$$0 < f_p < \frac{\delta_0 I_1 - f_c I_2(\Omega)}{I_5(\omega)},$$

then inequality (31) holds, it will imply $M(\theta_0) < 0$, in other words, the Melnikov function $M(\theta_0)$ has no zeros for any φ. Therefore, the parameter condition can be achieved for suppressing chaos.

Let

$$f_{po} = \frac{\delta I_1 - f_c I_2(\Omega)}{I_5(\omega)}, \tag{32}$$

the condition $0 < f_p < f_{po}$ implies $M(\theta_0)$ has no zeros for any φ. In other words, in the parameter interval $f_p \in (0,\ f_{po})$, the phase φ has no effect on suppressing chaotic motions.

Next we further study the suppression of chaos under the parameter condition $f_p > f_{po}$. If there exists positive integers m and n with reciprocal prime such that $\omega = m\Omega/n$, obviously, $M(\theta_0)$ is a periodic function in θ_0 with period $2\pi n/m\Omega$, we will get some subintervals that satisfy the following conditions.

Theorem 5. *If* $I_1 > 0$, $I_2(\Omega) > 0$, $I_5(\frac{m\Omega}{n}) > 0$ *and* $f_p > f_{po}$, *for any* $\theta_0 \in [0, 2\pi n/m\Omega]$, $\sin[(m\Omega/n)\theta_0]$ *and* $\sin(\Omega\theta_0)$ *satisfy the following inequalities:*

$$-\frac{f_{po}}{f_p} \leq \sin(\frac{m\Omega}{n}\theta_0) \leq 1 \tag{33}$$

$$-1 + \frac{(f_p - f_{po})I_5(\frac{m\Omega}{n})}{f_c I_2(\Omega)} \leq \sin(\Omega\theta_0) \leq 1 \tag{34}$$

then the Melnikov function $M(\theta_0) < 0$ *and the homoclinic chaos in system (9) can be suppressed for any phase* φ.

Proof: From the Eq. (29), we have:

$$\begin{aligned} M(\theta_0) =& -\delta I_1 - f_c I_2(\Omega)\sin\Omega\theta_0 - f_p \sin(\frac{m\Omega}{n}\theta_0 + \varphi)I_5(\frac{m\Omega}{n}) \\ \leq& -\delta I_1 + f_c I_2(\Omega)\cdot(1 - \frac{(f_p - f_{po})I_5(\frac{m\Omega}{n})}{f_c I_2(\Omega)}) + f_p I_5(\frac{m\Omega}{n})\frac{f_{po}}{f_p} \\ =& -\delta I_1 + f_c I_2(\Omega) + f_{po} I_5(\frac{m\Omega}{n}) - (f_p - f_{po})I_5(\frac{m\Omega}{n}) \\ =& -\delta I_1 + f_c I_2(\Omega) + \frac{\delta_0 I_1 - f_c I_2(\Omega)}{I_5(\frac{m\Omega}{n})} I_5(\frac{m\Omega}{n}) - (f_p - f_{po})I_5(\frac{m\Omega}{n}) \\ =& -(f_p - f_{po})I_5(\frac{m\Omega}{n}) < 0. \end{aligned} \tag{35}$$

then inequality holds, it will imply $M(\theta_0) < 0$, that is to say, the Melnikov function $M(\theta_0)$ has no zeros for any φ. Therefore, the parameter conditions can be achieved for suppressing chaos with parametric excitations.

4. Applications

We will employ the theorems obtained in the above section to study the suppression of chaotic motions for a concrete piecewise smooth oscillator subjected to weak damping and weak periodic external excitations. Illustrative examples are presented to show effectiveness of strategies for suppressing chaos based on the Melnikov analysis for the non-smooth oscillator. Finally, numerical evidences are further presented to verify the validity of methods of chaos control.

4.1. A piecewise smooth oscillator

The dynamical equation for a specific piecewise smooth oscillator is written of the form

$$\begin{cases} \dot{x} = y, \\ \dot{y} = \omega_0^2(\frac{1}{\alpha} - 1)x - 2\epsilon\mu y + \epsilon f_0 \cos\Omega t, & |x| < \alpha, \\ \dot{x} = y, \\ \dot{y} = -\omega_0^2(x - \text{sign}(x)) - 2\epsilon\mu y + \epsilon f_0 \cos\Omega t, & |x| > \alpha, \end{cases} \tag{36}$$

where $0 < \alpha < 1$, $\omega_0 > 0$, μ is the coefficient of damping, f_0 and Ω are respectively the amplitude and the frequency of the external excitations.

When the effect of damping and excitations is not considered, the unperturbed system obtained by letting $\epsilon = 0$ is a three-segment defined Hamiltonian system of the form

$$\begin{cases} \dot{x} = y = \frac{\partial H}{\partial y}, \\ \dot{y} = \omega_0^2(\frac{1}{\alpha} - 1)x = -\frac{\partial H}{\partial x}, & |x| < \alpha, \\ \dot{x} = y = \frac{\partial H}{\partial y}, \\ \dot{y} = -\omega_0^2(x - \text{sign}(x)) = -\frac{\partial H}{\partial x}, & |x| > \alpha, \end{cases} \tag{37}$$

where the Hamiltonian function is of the piecewise defined form

$$H(x,\,y)=\begin{cases} H_{-}(x,\,y)=\frac{1}{2}y^2+\frac{1}{2}\omega_0^2x^2-\frac{1}{2\alpha}\omega_0^2x^2, & |x|<\alpha,\\ H_{+}(x,\,y)=\frac{1}{2}y^2+\frac{1}{2}\omega_0^2x^2-\omega_0^2(\mathrm{sign(x)})x+\frac{1}{2}\omega_0^2\alpha, & |x|>\alpha \end{cases} \tag{38}$$

satisfying $H_{-}(\pm\alpha,\,y)$=$H_{+}(\pm\alpha,\,y)$.

From the unperturbed system (37), we can easily get three equilibrium state (0, 0), (1, 0) and (−1, 0), who belong to three different regions separated by the switching manifolds $\Sigma_{\pm}=\{(x,y)\in\mathbb{R}^2\mid x=\pm\alpha\}$. Simple calculation of eigenvalues of matrices at the three fixed points shows that the origin (0, 0) is a hyperbolic saddle-type point and lies in the region $V_c=\{(x,y)\in\mathbb{R}^2\mid -\alpha<x<\alpha\}$, and (±1, 0) are center-type fixed points withe pure imaginary eigenvalue and surrounded by piecewise-defined periodic orbits with arbitrary periods. Furthermore, there also exists piecewise defined a pair of solutions homoclinic to the origin (0, 0). The geometrical structure on the phase plane for the unperturbed system is similar to the Figure 4. We only analytically express the homoclinic orbit on the right side of $x=0$ of the form

$$\gamma(t)=\begin{cases} \gamma_{-}^1(t)=(e^{\lambda(t+T)},\,\lambda e^{\lambda(t+T)}), & for\ t\le -T,\\ \gamma_{+}(t)=(1+d\cos\omega_0 t,\,-\omega_0 d\sin\omega_0 t), & for\ -T\le t\le T,\\ \gamma_{-}^2(t)=(e^{-\lambda(t-T)},\,-\lambda e^{-\lambda(t-T)}), & for\ t\ge T, \end{cases} \tag{39}$$

where

$$\lambda=\omega_0\sqrt{\frac{1}{\alpha}-1},\ d=\sqrt{1-\alpha},\ T=\frac{1}{\omega_0}\arcsin(\frac{\alpha-1}{d}). \tag{40}$$

The Melnikov function is calculated by the formula (14) and is written as:

$$M(\theta_0)=-2\mu A(\alpha,\omega_0,\lambda,T)+f_0B(\alpha,\omega_0,\lambda,\Omega,T)\sin\Omega\theta_0, \tag{41}$$

where

$$A(\alpha,\omega_0,\lambda,T)=\lambda+d^2\omega_0^2(T-\frac{1}{2\omega_0}\sin 2\omega_0T)>0,$$

$$B(\alpha,\omega_0,\lambda,\Omega,T)=\frac{2\lambda}{\lambda^2+\Omega^2}(\lambda\sin\Omega T+\Omega\cos\Omega T)+d\omega_0(\frac{\sin(\omega_0-\Omega)T}{\omega_0-\Omega}-\frac{\sin(\omega_0+\Omega)T}{\omega_0+\Omega}).$$

We here note that the parameters d, T and λ involved in the above formula have been given in Eq.(40). We conclude that when the inequality

$$2\mu A(\alpha,\omega_0,\lambda,T)<f_0|B(\alpha,\omega_0,\lambda,\Omega,T)| \tag{42}$$

holds, the Melnikov function

$$M(\theta_0)=0 \tag{43}$$

possess a simple zero at some θ_0.

When the inequality is established, the threshold of the parameters for the existence of homoclinic chaos is analytically obtained. To illustrate the reliability of prediction by the Melnikov analysis, we first fix the parameter $\omega_0=1$. The detected chaotic threshold for system (36)for $\alpha=0.6$ and $\alpha=0.8$ is respectively plotted in Figure 5.

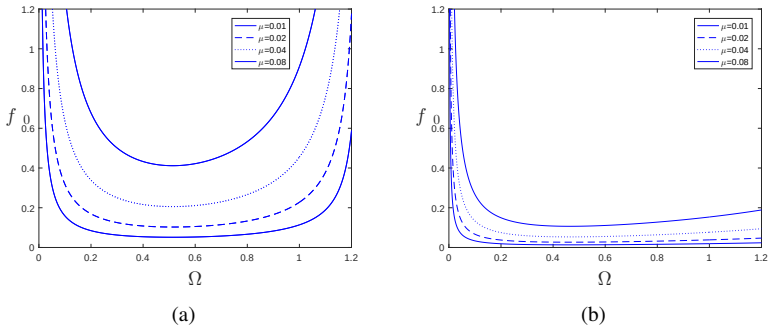

Figure 5: The chaotic threshold for system (36): (a) $\alpha=0.6$, (b) $\alpha=0.8$

Next we first fix $\Omega = 1.05$, and adjust α, μ and the amplitude of the excitation f_0 to facilitate the following analysis.

From the Fig. 5, for every fixed μ and α, if f_0 is in the region above the plotted curve as Ω varies, the Melnikov function $M(\theta_0)$ has a simple zero θ_0, which implies that homoclinic chaos will occur for system (36). The typical strange chaotic attractors with finger-like are demonstrated with $\alpha = 0.6$ and $f_0 = 0.82$ in Figure 6 for different damping. Figure 7 is the corresponding chaotic motions plotted in time process diagram. The damping is set to $\mu = 0.01$ in the Fig. 6(a) and Fig. 7(a), and the damping is $\mu = 0.08$ in the Fig. 6(b) and Fig. 7(b).

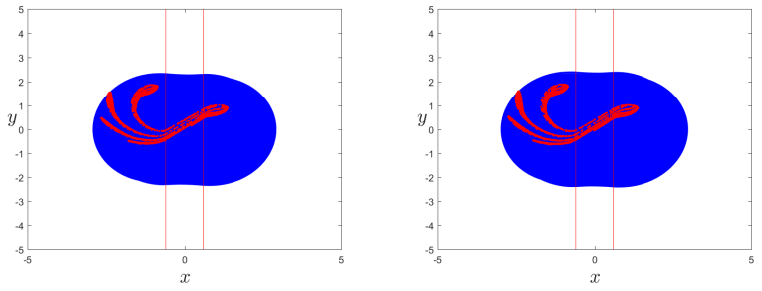

(a) (b)

Figure 6: Chaotic strange attractors with finger-like for system (36) with $\alpha = 0.6$ and $f_0 = 0.82$: (a) for $\mu = 0.01$, (b) for $\mu = 0.08$

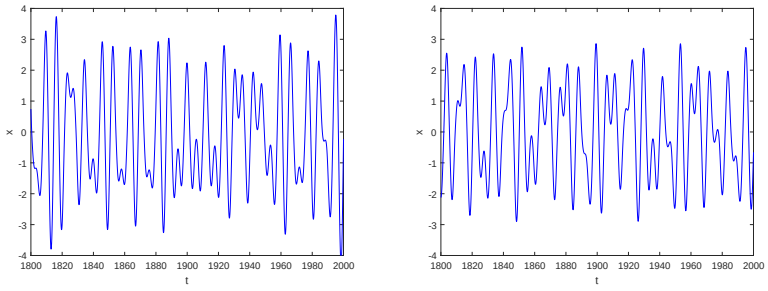

(a) (b)

Figure 7: Time process diagram for system (36) with $\alpha = 0.6$ and $f_0 = 0.82$:(a) for $\mu = 0.01$, (b) for $\mu = 0.08$

Similar numerical simulations, strange attractors and chaotic motions are also presented in Figure 8 and Figure 9 for $f_0 = 0.6$ and $\alpha = 0.8$ under different damping.

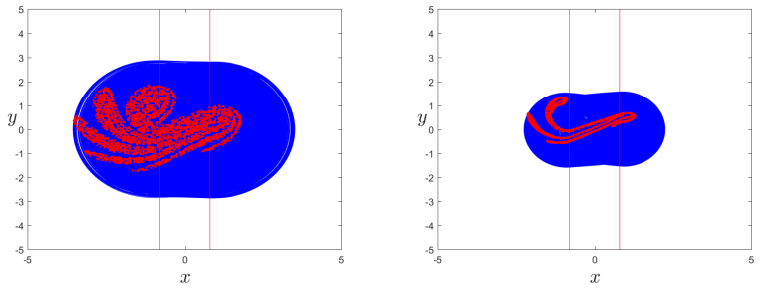

(a) (b)

Figure 8: Chaotic attractors for system (36) with $\alpha = 0.8$ and $f_0 = 0.6$: (a) for $\mu = 0.01$, (b) for $\mu = 0.08$

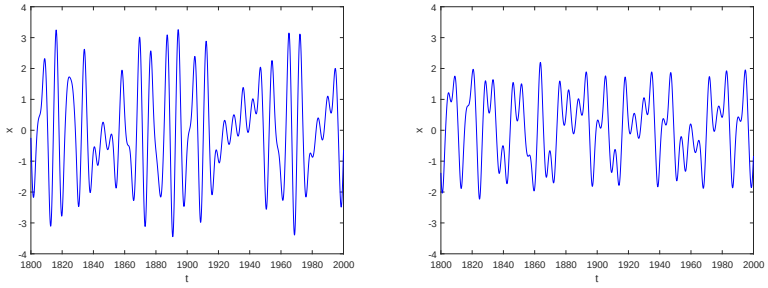

(a) (b)

Figure 9: Time process diagram for system (36) with $\alpha = 0.8$ and $f_0 = 0.6$: (a) for $\mu = 0.01$, (b) for $\mu = 0.08$

4.2. Adding state feedback control method

The weak velocity control signal $y(t)$ is a simple linear feedback to system (36), then the new system is

$$\begin{cases} \dot{x} = y, \\ \dot{y} = \omega_0^2(\frac{1}{\alpha} - 1)x - 2\epsilon\mu y + \epsilon f_0 \cos\Omega t - \epsilon E y, & |x| < \alpha, \end{cases}$$
$$\begin{cases} \dot{x} = y, \\ \dot{y} = -\omega_0^2(x - \text{sign}(x)) - 2\epsilon\mu y + \epsilon f_0 \cos\Omega t - \epsilon E y, & |x| > \alpha, \end{cases} \tag{44}$$

where $-\epsilon E y$ indicates weak damping force. After a series calculations, the corresponding Melnikov function is

$$M(\theta_0) = (-2\mu - E)A(\alpha, \omega_0, \lambda, T) + f_0 B(\alpha, \omega_0, \lambda, \Omega, T)\sin\Omega\theta_0, \tag{45}$$

If the inequality

$$(2\mu + E)A(\alpha, \omega_0, \lambda, T) > f_0|B(\alpha, \omega_0, \lambda, \Omega, T)| \tag{46}$$

holds, it can be seen that for any θ_0

$$M(\theta_0) \neq 0, \tag{47}$$

that is $M(\theta_0)$ has no zeros. Hence the above Melnikov analysis provide us with a good idea to only adjust the parameter E of the linear feedback such that inequality (46) holds. Thus chaotic behavior in the system (36) will be suppressed through the aforementioned state feedback control method.

Through the non-smooth Melnikov analysis, the threshold curve for the linear state feedback with different damping is respectively shown in Figure 10 for two sets of parameters $\alpha = 0.6$, $f_0 = 0.82$ and $\alpha = 0.8$, $f_0 = 0.6$. For every fixed damping μ, if E is in the zone above the plotted curve as Ω varies, then the homoclinic chaos exhibited in the Fig. 6 and Fig. 8 under given initial conditions will be suppressed for system (36).

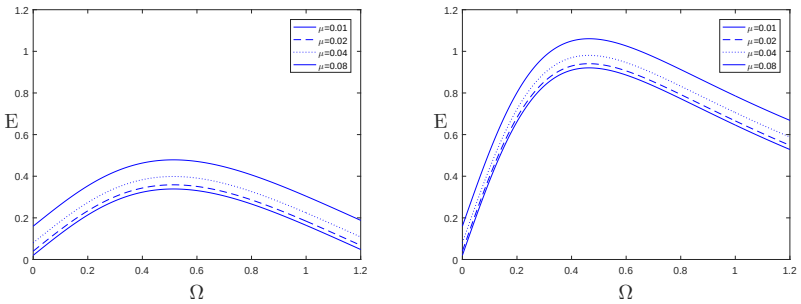

(a) (b)

Figure 10: The thresholds of parameters for system (44) with state feedback control, (a) for $\alpha = 0.6$, $f_0 = 0.82$, (b) for $\alpha = 0.8$, $f_0 = 0.6$.

In addition to adjusting the state feedback E, the initial conditions and system parameters used in the Fig. 6 and Fig. 7 have not been changed. Periodic motions are demonstrated in Figure 11 and Figure 12 with $\alpha = 0.6$ and $f_0 = 0.82$ to show the effectiveness in suppressing chaotic attractors in the Fig. 6 by the state feedback control. The periodic motion only crosses the switching manifold $\Sigma_+ = \{(x, y) \in \mathbb{R}^2 \mid x = \alpha\}$ and the control parameter is chosen as $E = 1.3$ in the Fig. 11(a) and Fig. 12(a) with the damping $\mu = 0.01$, and we also adjust the control parameter to $E = 0.5$ in the Fig.11(b) and Fig. 12(b) such that the periodic motion crosses through two switching manifolds where the damping is $\mu = 0.08$.

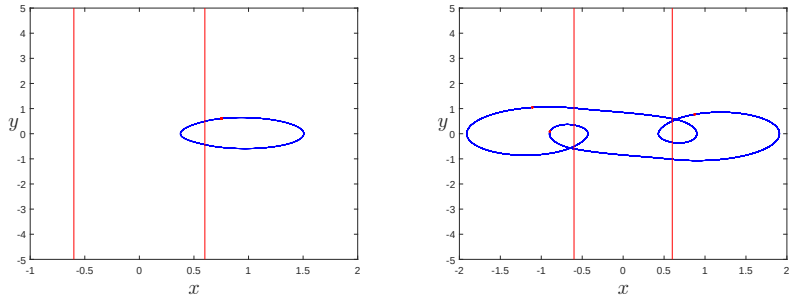

(a) (b)

Figure 11: Controlled period motions for system (44) with $\alpha = 0.6$ and $f_0 = 0.82$: (a) for $\mu = 0.01, E = 1.3$, (b) for $\mu = 0.08, E = 0.5$.

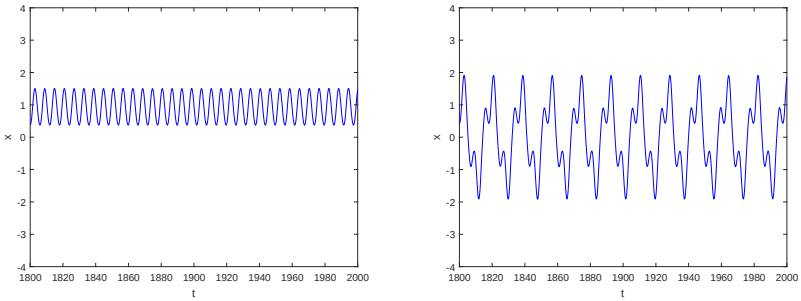

(a) (b)

Figure 12: Time process diagram for state feedback control system (44) with $\alpha = 0.6$ and $f_0 = 0.82$: (a) for $\mu = 0.01, E = 1.3$, (b) for $\mu = 0.08, E = 0.5$.

Similar periodic motions crossing only one of the two switching manifolds $\Sigma_\pm = \{(x, y) \in \mathbb{R}^2 \mid x = \pm\alpha\}$ are generated in Figure 13 and Figure 14 by adjusting the state feedback E such that the chaotic motions shown in the Fig.7 are suppressed for $\alpha = 0.8$ and $f_0 = 0.6$. The control parameter is $E = 0.85$ in the Fig.13(a) and the Fig. 14(a) for the damping $\mu = 0.01$, and the state feedback E is chosen as $E = 0.9$ in the Fig.13(b) and the Fig. 14(b) for the damping $\mu = 0.08$.

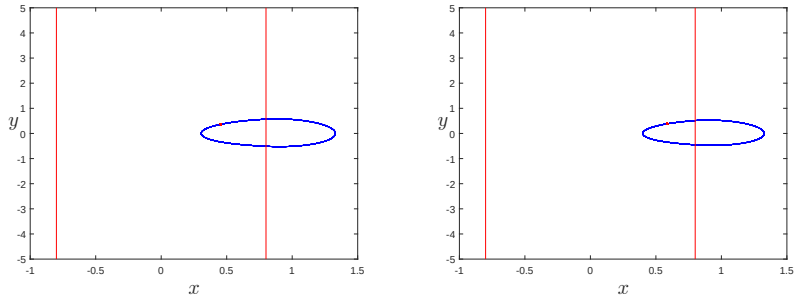

(a) (b)

Figure 13: Controlled period motions for system (44) with $\alpha = 0.8$ and $f_0 = 0.6$: (a) $E = 0.85$, $\mu = 0.01$,, (b) $E = 0.9$, $\mu = 0.08$.

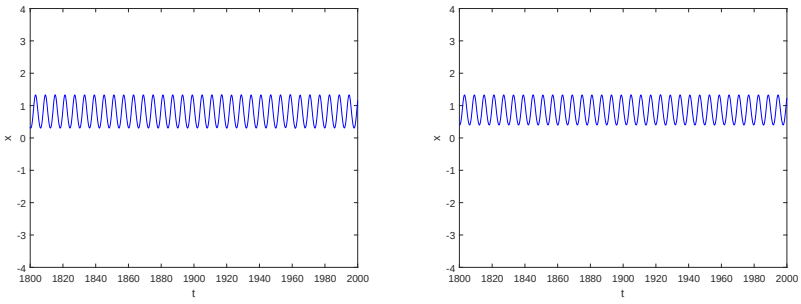

(a) (b)

Figure 14: Time process diagram for system (44) with $\alpha = 0.8$ and $f_0 = 0.6$: (a) $E = 0.85$, $\mu = 0.01$,, (b) $E = 0.9$, $\mu = 0.08$,.

4.3. Adding self-adaptive control method

Assume that the parameter μ implements to the self-adaptive control

$$\dot{\mu} = -2Px(t)\dot{x}(t)$$

i.e.

$$\mu = \mu_0 - Px^2(t) \tag{48}$$

The system with self-adaptive control is written of the form

$$\begin{cases} \dot{x} = y, \\ \dot{y} = \omega_0^2(\frac{1}{\alpha} - 1)x - 2\epsilon(\mu_0 - Px^2)y + \epsilon f_0 \cos\Omega t, & |x| < \alpha \\ \dot{x} = y, \\ \dot{y} = -\omega_0^2(x - \text{sign}(x)) - 2\epsilon(\mu_0 - Px^2)y + \epsilon f_0 \cos\Omega t, & |x| > \alpha. \end{cases} \tag{49}$$

Similar Melnikov analysis yields

$$M(\theta_0) = -2\mu_0 A(\alpha, \omega_0, \lambda, T) + f_0 B(\alpha, \omega_0, \lambda, \Omega, T)\sin\Omega\theta_0 + PC(\alpha, \omega_0, \lambda, T). \tag{50}$$

where

$$C(\alpha, \omega_0, \lambda, T) = \lambda + 2d^2\omega_0^2(T - \frac{1}{2\omega_0}sin2\omega_0 T) + \frac{8}{3}d^3\omega_0 sin^3\omega_0 T + \frac{1}{2}\omega_0^2 d^4 T - \frac{1}{8}\omega_0^2 d^4 sin4\omega_0 T.$$

The damping μ_0 can be seen as the same value of damping given in advance in the Figure 6 and the Figure 8 for the existence of chaotic attractors. If the self-adaptive control parameter P satisfies the following parametric inequality:

$$f_0|B(\alpha, \omega_0, \lambda, \Omega, T)| < |2\mu_0 A(\alpha, \omega_0, \lambda, T) - PC(\alpha, \omega_0, \lambda, T)|, \tag{51}$$

then for any θ_0

$$M(\theta_0) \neq 0,$$

which implies that chaotic motion can be suppressed by adding self-adaptive control.

Through the non-smooth Melnikov analysis, the threshold curve of self-adaptive control method is obtained as shown in Figure 15 for two sets of parameters $\alpha = 0.6$, $f_0 = 0.82$ and $\alpha = 0.8$, $f_0 = 0.6$ respectively, and other parameters remain unchanged.

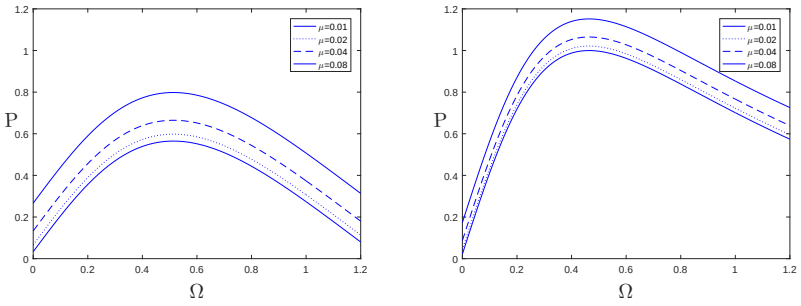

Figure 15: The thresholds of parameters for system (49) by adding self-adaptive control method , (a) for $\alpha = 0.6$, $f = 0.82$ (b) for $\alpha = 0.8$, $f = 0.6$

From the Fig. 15, for every fixed damping μ and the parameter α, if P is in the zone above the plotted curve as Ω varies, then the homoclinic chaos shown in the Fig.6 and the Fig.8 will be suppressed for system (36). Periodic motions are demonstrated from the Figure 16 to the Figure 19 to verify the feasibility of the presented self-adaptive control, and the homoclinic chaos is suppressed only by adjusting the control parameter P.

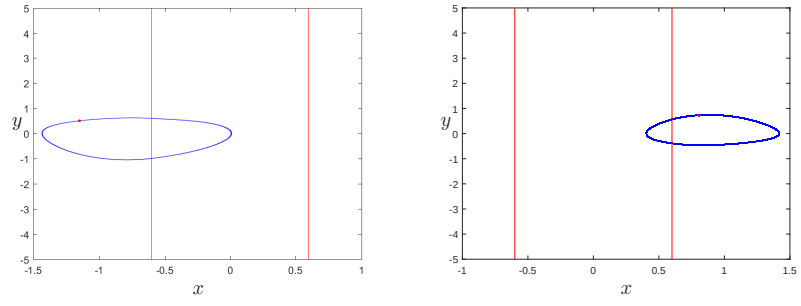

Figure 16: Controlled period motions for system (49) with $\alpha = 0.6$ and $f_0 = 0.82$: (a) $\mu = 0.01, P = 0.5$, (b) $\mu = 0.08, P = 0.7$.

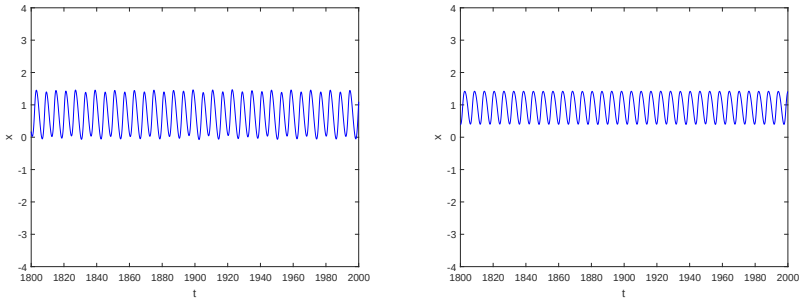

(a) (b)

Figure 17: Time process diagram for self-adaptive control system (49) with $\alpha = 0.6$ and $f_0 = 0.82$: (a) $\mu = 0.01, P = 0.5$, (b) $\mu = 0.08, P = 0.7$.

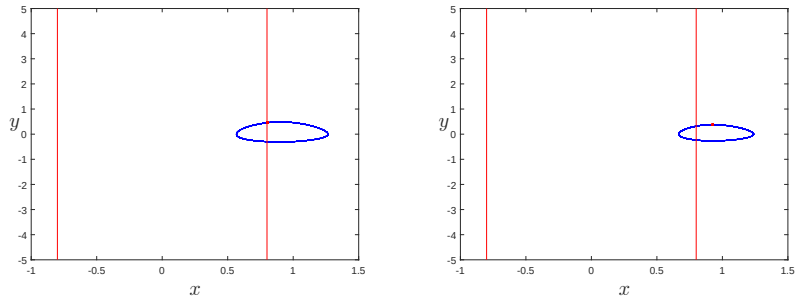

(a) (b)

Figure 18: Controlled period motions for system (49) with $\alpha = 0.8$ and $f_0 = 0.6$: (a) $\mu = 0.01, P = 0.85$, (b) $\mu = 0.08, P = 0.95$.

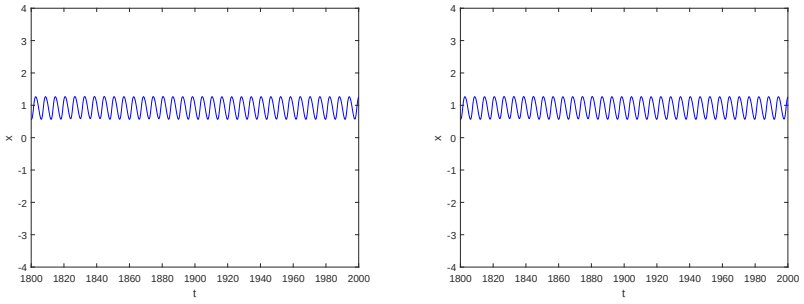

(a) (b)

Figure 19: Time process diagram for self-adaptive control system (49) with $\alpha = 0.8$ and $f_0 = 0.6$: (a) $\mu = 0.01, P = 0.85$, (b) $\mu = 0.08, P = 0.95$.

4.4. Control of chaos with adding parametric excitations

The controlled system with parametric excitations is rewritten as:

$$\begin{cases} \dot{x} = y, \\ \dot{y} = \omega_0^2(\frac{1}{\alpha} - 1)x - 2\epsilon\mu y + \epsilon f_0 \cos\Omega t + \epsilon x f_p \cos(\omega t + \varphi), & |x| < \alpha, \\ \dot{x} = y, \\ \dot{y} = -\omega_0^2(x - \text{sign}(x)) - 2\epsilon\mu y + \epsilon f_0 \cos\Omega t + \epsilon x f_p \cos(\omega t + \varphi), & |x| > \alpha, \end{cases} \tag{52}$$

where f_p, ω and , φ respectively denote the amplitude, frequency, initial phase of control excitation, respectively. By similar mathematical technique, the corresponding Melnikov function is obtained of the form

$$M(\theta_0) = -2\mu A(\alpha, \omega_0, \lambda, T) + f_0 B(\alpha, \omega_0, \lambda, \Omega, T)\sin\Omega\theta_0 + f_p D(\alpha, \omega_0, \lambda, \omega, T)\sin(\omega\theta_0 + \varphi), \tag{53}$$

where

$$\begin{aligned} D(\alpha, \omega_0, \lambda, \omega, T) =& \frac{4\lambda^2 \sin\omega T + 2\omega\lambda\cos\omega T}{4\lambda^2 + \omega^2} + d\omega_0[\frac{\sin(\omega_0 - \omega)T}{\omega_0 - \omega} - \frac{\sin(\omega_0 + \omega)T}{\omega_0 + \omega}] \\ &+ \frac{1}{2}d^2\omega_0[\frac{\sin(2\omega_0 - \omega)T}{2\omega_0 - \omega} - \frac{\sin(2\omega_0 + \omega)T}{2\omega_0 + \omega}]. \end{aligned} \tag{54}$$

Based on the Theorem 4 in Section 3, we can obtain the parameter condition

$$0 < f_p < \frac{2\mu A(\alpha, \omega_0, \lambda, T) - f_0|B(\alpha, \omega_0, \lambda, \Omega, T)|}{|D(\alpha, \omega_0, \lambda, \omega, T)|}, \tag{55}$$

such that for any θ_0 and control phase φ

$$M(\theta_0) < 0,$$

which implies that chaotic motion can be suppressed by adding the parametric excitation.

Through the Melnikov analysis, the threshold curve of adding parametric excitations control is obtained as shown in Figure 20 for two sets of parameters $\alpha = 0.6$, $f_0 = 0.82$ and $\alpha = 0.8$, $f_0 = 0.6$ respectively, and other parameters remain unchanged.

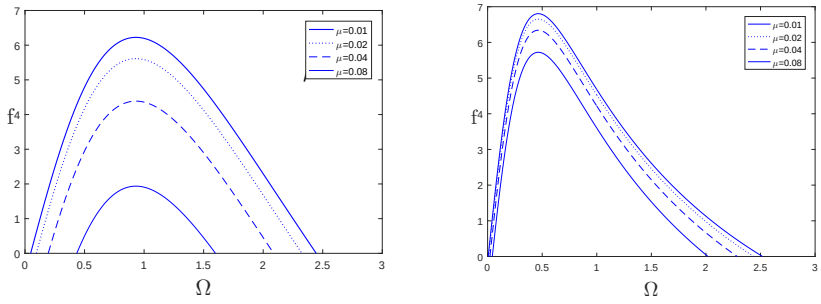

(a) (b)

Figure 20: The thresholds of parameters for system (52) with parametric excitations. (a) for $\alpha = 0.6$, $f_0 = 0.82$, (b) for $\alpha = 0.8$, $f_0 = 0.6$.

From the Fig.20, for every fixed damping μ and the parameter α, if f_p is in the zone above the plotted curve as Ω varies, then homoclinic chaos will be suppressed for system (36) only by adjusting the amplitude f_p of the parametric excitation.

We first fix $\omega_0 = 1$, $\Omega = \omega = 1.05$, $\mu = 0.08$ in the following analysis. Two sets of parameters are respectively set to $\alpha = 0.6, f_0 = 0.82$ and $\alpha = 0.8, f_0 = 0.6$ to ensure that the Melnikov's function $M(\theta_0)$ has no zeros. Very rich periodic motions crossing the switching manifolds are demonstrated from Figure 21 to Figure 24 to state the effectiveness for suppressing chaos by adjusting the control parameter f_p of the parametric excitations.

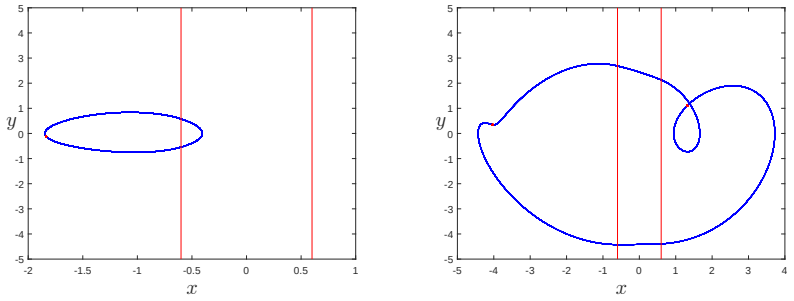

(a) (b)

Figure 21: Controlled period motions for system (52) with $\alpha = 0.6, \mu = 0.08$: (a) $f_p = 0.6$, (b) $f_p = 0.98$.

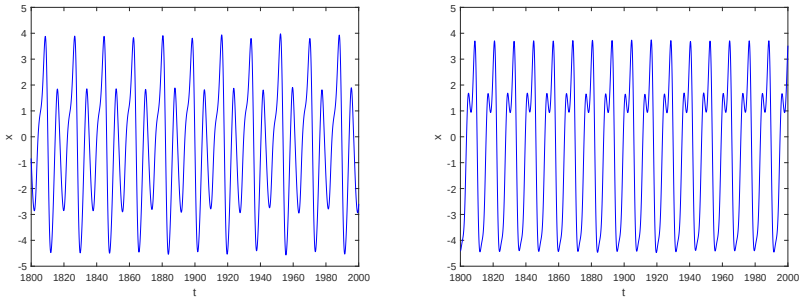

(a) (b)

Figure 22: Time process diagram for system (52) with $\alpha = 0.6$, $f_0 = 0.82$: (a) $f_p = 0.6$, (b) $f_p = 0.98$.

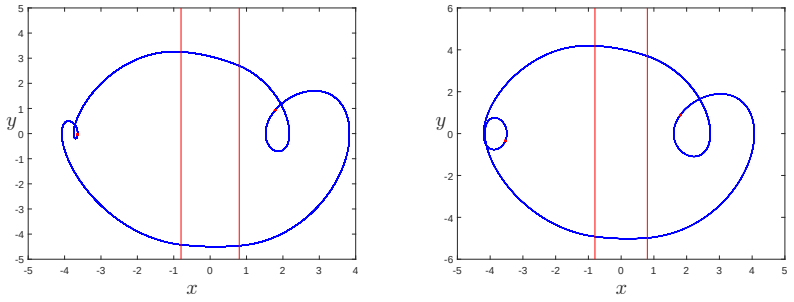

(a) (b)

Figure 23: Controlled period motions for system (52) with $\alpha = 0.8$, $f_0 = 0.6$: (a) for $f_p = 1.1$, (b) for $f_p = 1.28$.

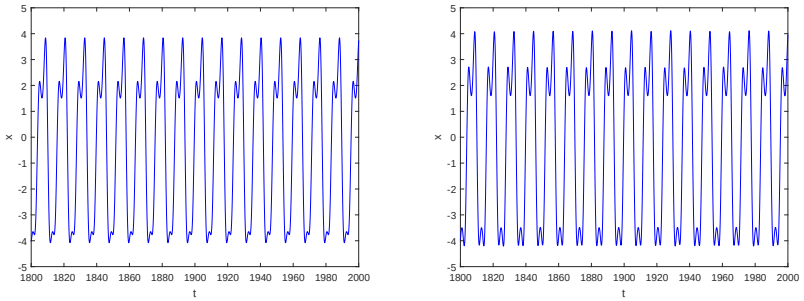

(a) (b)

Figure 24: Time process diagram for system (52) with $\alpha = 0.8, \mu = 0.08$: (a) for $f_p = 1.1$, (b) for $f_p = 1.28$.

5. Conclusions

In this paper, we present some simple and easily accessible control methods of homoclinic chaos for a non-smooth oscillator with weak time-periodic perturbation. The key idea is to modify slightly the Melnikov function such that the zeros of the function are eliminated through additional controls, namely, state feedback control, self-adaptive control and parametric excitations control. This paper gives a general form of planar piecewise smooth oscillators, which often be seen as an ideal model to approximate many nonlinear restoring force of smooth oscillators under all kinds of damping effects and periodic excitations. The unperturbed system is assumed to has a pair of homoclinic solutions with piecewise smooth, which transversally cross through switching manifolds. Then, the Melnikov analysis is employed to detect the threshold of parameters for homoclinic chaos in the perturbed system with damping and excitations. When some methods of state feedback control, self-adaptive control and parametric excitations control are respectively considered, detailed Melnikov analysis and sufficient criteria for suppressing homoclinic chaos are analytically derived. Finally, sufficient criteria are obtained to study the control of homoclinic chaos through a concrete piecewise smooth oscillator. Numerical simulations are also presented to verify the validity of suppressing chaos by the analytical Melnikov method for non-smooth oscillators.

Acknowledgments

The authors gratefully acknowledge the support of the National Natural Science Foundation of China (NNSFC) through Grant Nos. 11672326, 11802208, 11602210, U1533103.

Compliance with Ethical Standards

Funding: This study was founded by the National Natural Science Foundation of China through Grant Nos. 11672326, 11802208, 11602210, U1533103.

Conflict of Interest: The authors declare that they have no conflict of interest.

References

[1] Budd, C. J.: Non-smooth dynamical systems and the grazing bifurcation. Nonlinear mathematics and its applications, 219-235 (1996)
[2] Kunze, M. Non-smooth dynamical systems. Springer-Verlag, Berlin (2000)
[3] Cao, Q., Wiercigroch, M., Pavlovskaia, E. E., Grebogi, C., Thompson, J. M. T.: Archetypal oscillator for smooth and discontinuous dynamics. Physical Review E. **74**, 046218 (2006)
[4] Bernardo, M. D., Budd, C. J., Champneys, A. R., Kowalczyk, P.: Piecewise-smooth dynamical systems: theory and application. Springer-Verlag, London (2008)
[5] Leine, R.I., Van Campen, D.H., Van de Vrande, B.L.: Bifurcations in nonlinear discontinuous systems. Nonlinear Dyn. **23**, 105-164 (2000)
[6] Feldbrugge, J., Lehners, J. L., Turok, N.: No smooth beginning for spacetime. Physical review letters. **119**171301 (2017)
[7] Pei, J. S., Wright, J. P., Gay-Balmaz, F., Beck, J. L., Todd, M. D.: On choosing state variables for piecewise-smooth dynamical system simulations. Nonlinear Dynamics, 1-24(2018)

[8] Nesterov, Y.: Excessive gap technique in nonsmooth convex minimization. SIAM Journal on Optimization **16**, 235-249 (2005)
[9] Nordmark, A. B.: Non-periodic motion caused by grazing incidence in an impact oscillator. Journal of Sound and Vibration, 279-297(1991)
[10] Popp, K., and Stelter,P.: Nonlinear oscillations of structures induced by dry friction. Nonlinear dynamics in engineering systems. Springer, Berlin, Heidelberg, 233-240(1990)
[11] Kobori, T., Takahashi, M., Nasu, T., Niwa, N., Ogasawara, K.: Seismic response controlled structure with active variable stiffness system. Earthquake engineering structural dynamics, 925-941(1993)
[12] Adler, D., Henisch, H. K., Mott, N.: The mechanism of threshold switching in amorphous alloys. Reviews of Modern Physics, 209(1978)
[13] Mackey, M. C., Glass, L.: Oscillation and chaos in physiological control systems. Science. **197**, 287-289(1977)
[14] Hefner, A. R., Blackburn, D. L.: Simulating the dynamic electro-thermal behavior of power electronic circuits and systems. In [Proceedings] 1992 IEEE Workshop on Computers in Power Electronics, 143-151(1992)
[15] Chen, G., Yu, X. ,Eds.: Chaos control: theory and applications. Springer Science Business Media.**292**, (2003)
[16] Ott, E., Grebogi, C., Yorke, J. A.: Controlling chaos. Physics Review Letters. **64**, 1196-1199(1990)
[17] Pyragas, K.: Control of chaos via extended delay feedback. Physics letters A. **206**, 323-330(1995)
[18] Gritli, H., Belghith, S. Walking dynamics of the passive compass-gait model under OGY-based control: emergence of bifurcations and chaos. Communications in Nonlinear Science and Numerical Simulation. **47**,308-327(2017)
[19] Ling, Y., Liu, Z. R.: An improvement and proof of OGY method. Applied Mathematics and Mechanics. **19**, 1-8(1998)
[20] de Paula, A. S., Savi, M. A.: A multiparameter chaos control method based on OGY approach. Chaos, Solitons and Fractals. **40**, 1376-1390(2009)
[21] Parthasarathy, S., Sinha, S.: Controlling chaos in unidimensional maps using constant feedback. Physical Review E, **51**, 6239(1995)
[22] Osipov, G. V., Kozlov, A. K., Shalfeev, V. D.: Impulse control of chaos in continuous systems. Physics Letters A. **247**, 119-128(1998)
[23] Qu, Z.L., Hu, G., Yang, G.J., Qin, G.R.: Phase effect in taming nonautonomous chaos by weak harmonic perturbations. Physical Review Letters. **74**, 1736C1739(1995)
[24] Meucci, R., Gadomski, W., Ciofini, M., Arecchi, F. T.: Experimental control of chaos by means of weak parametric perturbations. Physical Review E. **49**, R2528 (1994)
[25] Meucci, R., Euzzor, S., Pugliese, E., Zambrano, S., Gallas, M. R., Gallas, J. A. C.: Optimal phase-control strategy for damped-driven Duffing oscillators. Physical review letters. **116** 044101 (2016)
[26] Hubler, A. W.: Adaptive control of chaotic system. Helv Phys Acta.**62**, 343-346(1989)
[27] Braiman, Y., Goldhirsch, I.: Taming chaotic dynamics with weak periodic perturbations. Physical Review Letters. **66**, 2545-2548(1991)
[28] Melnikov, V. K.: On the stabiity of the center for time periodic perturbations. Tans. Moscow Math. Soc. **12**, 1-57 (1963)
[29] Guckenheimer, J., Holmes, P.: Nonlinear oscillations, dynamical system and bifurcations of vector fields. Springer, New York (1983)
[30] Wiggins, S.: Global bifurcations and chaos-analytical methods. Springer, New York (1988)
[31] Zhang, W., Zhang, J. H., Yao, M. H.: The extended Melnikov method for non-autonomous nonlinear dynamical systems and application to multi-pulse chaotic dynamics of a buckled thin plate. Nonlinear Analysis: Real World Applications. **11**, 1442-1457 (2010)
[32] Yao, M. H., Zhang, W., Zu, J. W.: Multi-pulse Chaotic dynamics in non-planar motion of parametrically excited viscoelastic moving belt. Journal of Sound and Vibration. **331**, 2624-2653 (2012)
[33] Kukučka, P.: Melnikov method for discontinuous planar sytems.: Nonlinear Analysis Theory Methods and Applications. **66**, 2698-2719 (2007)
[34] Shi, L., Zou, Y., Tassilo Kpper.: Melnikov method and detection of chaos for non-smooth systems. Acta Mathematicae Applicatae Sinica, English Series. **29**, 881-896 (2013)
[35] Du, Z. D, Zhang, W. N: Melnikov method for homoclinic bifurcations in nonlinear impact oscillators. Computers and Mathematics with Applications **50**, 445-458 (2005)
[36] Xu, W., Feng, J. Q, Rong, H. W: Melnikov's method for a general nonlinear vibro-impact oscillator. Nonlinear Analysis: Theory, Methods and Applications. **71**, 418-426 (2009)
[37] Granados, A., Hogan, S. J., Seara, T. M.: The Melnikov Method and Subharmonic Orbits in a Piecewise-Smooth System. SIAM J. Appl. Dyn. Syst. **11**, 801-830 (2012)
[38] Battelli, F., Fečkan, M.: Homoclinic trajectories in discontinuous systems. Journal of Dynamics and Differential Equations. **20**, 337-376 (2008)
[39] Battelli, F., Fečkan, M.: Bifurcation and chaos near sliding homoclinics. Journal of Differential Equations. **248**, 2227-2262 (2010)
[40] Battelli, F., Fečkan, M.: Nonsmooth homoclinic orbits, Melnikov functions and chaos in discontinuous systems. Physica D. **241**, 1962-1975 (2012)
[41] Tian, R. L., Zhou, Y. F., Zhang, B. L., Yang, X. W.: Chaotic threshold for a class of impulsive differential system. Nonlinear Dynamics. **83**, 2229-2240 (2016)
[42] Li, S.B., Zhang, W., Hao, Y.X.: Melnikov-type method for a class of discontinuous planar systems and applications. Int. J. Bifur. and Chaos. **24**, (1450022), 1-18 (2014)
[43] Li, S. B., Shen, C., Zhang, W., Hao, Y. X.: Homoclinic bifurcations and chaotic dynamics for a piecewise linear system under a periodic excitation and a viscous damping. Nonlinear Dyn. **79**, 2395-2406 (2015)
[44] Li, S. B., Ma, W. S., Zhang, W., Hao, Y. X. : Melnikov method for a three-zonal planar hybrid piecewise-smooth system and application. Int. J. Bifur. and Chaos. **26**, 1650014, 1-13 (2016)
[45] Li, S. B., Ma, W. S., Zhang, W., Hao, Y. X. : Melnikov method for a class of planar hybrid piecewise-smooth systems. Int. J. Bifur. and Chaos. **26** , 1650030, 1-12 (2016)
[46] Li, S. B., Gong, X. J., Zhang, W., Hao, Y. X.: The Melnikov method for detecting chaotic dynamics in a planar hybrid piecewise smooth system with a switching Manifold. Nonlinear Dyn. **89**, 939-953 (2017)
[47] Li, S. B., Zhao, S. B.: The analytical method of studying subharmonic periodic orbits for planar piecewise smooth systems with two switching manifolds. International Journal of Dynamics and Control. 1-13 (2018)
[48] Lima, R., Pettini, M.: Suppression of chaos by resonant parametric perturbations. Physical Review A, **41**, 726 (1990)

[49] Rajasekar, S.: Controlling of chaos by weak periodic perturbations in Duffing-van der Pol oscillator. Pramana. bf 41, 295-309 (1993)
[50] Lenci, S. Rega, G.: Optimal control of nonregular dynamics in a Duffing oscillator, Nonlinear Dyn. **33**, 71C86 (2003)
[51] Andrew, Y. T. L., Liu, Z. R.: Suppressing chaos for some nonlinear oscillators. Int. J. Bifur. and Chaos. **14**, 1455-1465(2004)
[52] Andrew, Y. T. L., Liu, Z. R.: Some new methods to suppress chaos for a kind of nonlinear oscillator. Int. J. Bifur. and Chaos. **14**, 2955-2961(2004)
[53] Chacón, R.: Control of Homoclinic Chaos by Weak Periodic Perturbations. World Scientific, London (2005)
[54] Yang, J., Jing, Z.: Controlling chaos in a pendulum equation with ultra-subharmonic resonances. Chaos, Solitons and Fractals. **42**, 1214-1226 (2009)
[55] Jimenez-Triana, A., Tang, W. K. S., Chen, G., Gauthier, A.: Chaos control in Duffing system using impulsive parametric perturbations. IEEE Transactions on Circuits and Systems II: Express Briefs. **57**, 305-309 (2010).
[56] Li, H., Liao, X., Huang, J., Chen, G., Dong, Z., Huang, T.: Diverting homoclinic chaos in a class of piecewise smooth oscillators to stable periodic orbits using small parametrical perturbations. Neurocomputing. **149**, 1587-1595 (2015)
[57] Du, L., Zhao, Y. P, Lei, Y. M,Hu, J., Yue, X.: Suppression of chaos in a generalized Duffing oscillator with fractional-order deflection, Nonlinear Dyn. **92**, 1921C1933 (2018)
[58] Martínez Ovejas, P. J., Euzzor, S., Gallas, J. A. C., Meucci, R., Chacón García, R.: Identification of minimal parameters for optimal suppression of chaos in dissipative driven systems. Scientific reports. **7**, 17988 (2017)
[59] Chacón, R., Miralles, J. J., Martínez, J. A., Balibrea, F.: Taming chaos in damped driven systems by incommensurate excitations. Communications in Nonlinear Science and Numerical Simulation. **73** 307-318 (2019)
[60] Shaw, S. W., Holmes, P. J.: A periodically forced piecewise linear oscillator. Journal of sound and vibration. **90**, 129-155 (1983)
[61] Cao, Q.J, Wiercigroch, M., Pavlovskaia, E. E., Thompson, J. M. T., Grebogi, C.: Piecewise linear approach to an archetypal oscillator for smooth and discontinuous dynamics. Philosophical Transactions of the Royal Society A: Mathematical, Physical and Engineering Sciences. **366**, 635-652 (2007)
[62] Lai, S. K., Wu, B. S., Lee, Y. Y.: Free vibration analysis of a structural system with a pair of irrational nonlinearities. Applied Mathematical Modelling. **45**, 997-1007 (2017)